

# Chapter 4

## Interaction of phloretin with membranes: On the mode of action of phloretin at the water-lipid interface

### 4.1 Abstract

The interaction of phloretin with single bilayers on a spherical support and with multilamellar vesicles was studied by differential scanning calorimetry (DSC) and nuclear magnetic resonance (NMR). The results of the methods applied indicate that phloretin strongly interacts with the lipid layer and changes its structural parameters. In DSC experiments phloretin in its neutral form strongly decreases phase transition temperature and slightly reduces cooperativity of phase transition within the lipid layer. In NMR measurements phloretin leads to an increase of the transverse relaxation time but has no effect on the spin lattice relaxation time. Computational conformational analysis of phloretin in the gas phase showed a wide distribution of the dipole moments of phloretin conformers, which mainly depend on the orientation of the OH moieties. The overall dipole moment of phloretin was calculated and experimentally determined. In both cases it is roughly 40% lower than has been published previously. This result suggests that the size of the dipole moment of phloretin does not provide such a high contribution to the effect of phloretin on the dipole potential of monolayers and bilayers as has been published previously. The adsorption of phloretin as determined from its binding to solid supported bilayers differs from the one determined from dipole potential measurements on black lipid membranes. The difference between the phloretin dissociation constants of both types of experiments suggests a change of its dipole moment normal to the membrane surface in a concentration dependent manner.

## 4.2 Introduction

The effects of phloretin (Fig. 4.1) on natural and artificial membranes deal in most cases with changes of the conductance for ions and the permeability for a number of neutral solutes (LeFevre and Marshall, 1959; Macey and Farmer, 1970; Toon and Solomon, 1987; Jennings and Solomon, 1976; Forman et al., 1982; Gunn et al., 1975; Owen, 1974; Verkman and Solomon, 1982). These changes are mainly attributed to the phloretin-induced change of dipole potential of the membranes. Phloretin in its neutral form decreases the dipole potential of membranes and lipid monolayers by the introduction of dipoles aligned opposite to those of the lipid molecules (Andersen et al., 1976; Melnik et al., 1977; Reyes et al., 1983; Cousin and Motais, 1978, Cseh and Benz, 1998).

Besides the electric effects discussed in the literature in detail, phloretin should also affect structural parameters of lipid membranes. Due to the ability of phloretin to adsorb to membranes and lipid monolayers, a strong influence on structural properties, in particular on lipid packing and phase transition can be expected as effects of hydrophobic interactions between lipids and phloretin. Of further interest is the examination of the structure of the phloretin molecule with respect to the possible variation of its conformers and their dipole moments since the dipole potential reducing effect of phloretin is mainly attributed to its large dipole moment (Andersen et al., 1976, Reyes et al., 1983; Cseh and Benz, 1998). The phloretin effect on structural properties of membranes and monolayers together with results of electric measurements should permit a much better understanding of the interaction of phloretin with membranes.

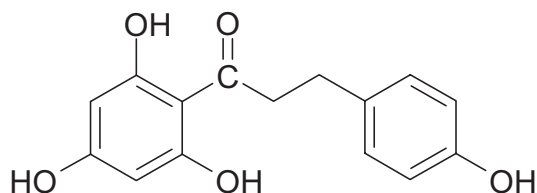


**FIGURE 4.1** Structural formula of phloretin (3-[4 hydroxyphenyl]-1-[2,4,6-trihydroxyphenyl]-1-propanone).

In this study we investigated the effects of phloretin on structural properties of lipid membranes using different methods. Information about the phloretin-mediated change of molecular order of lipid layers were gained by differential scanning calorimetry (DSC). DSC is well established as a method to study phase transition temperature, excess enthalpy and cooperativity of lipid bilayers and multilamellar lipid vesicles (MLV) (McElhaney, 1982; Naumann et al., 1992; Biltonen and Lichtenberg, 1993). Interaction of MLVs with surface active substances such as phloretin may cause changes of the phase transition temperature. According to an increase/decrease of the phase transition temperature and the change of the shapes of the heat capacity curves it is possible to estimate the quality and quantity of the lipid-phloretin interaction.

Spherical supported unilamellar lipid vesicles (SSV) were used to directly measure the physical parameters of phloretin adsorption in a quantitative way. Adsorption of phloretin, often determined only by the phloretin-induced dipole potential change (Reyes et al., 1983; De Levie et al. 1979; Cseh and Benz, 1998), can also be gained by this method and provides additional information about the saturation behavior of phloretin on membranes. We determined the characteristic adsorption parameters on the basis of a Langmuir adsorption isotherm. By comparison with the adsorption isotherm determined by measurements of the dipole potential change (Reyes et al., 1983; De Levie et al. 1979; Cseh and Benz, 1998) we obtained information whether phloretin adsorption is accompanied by possible structural changes and dipole rearrangements.

In another set of experimental conditions we employed Deuterium-NMR spectroscopy ( $^2\text{H}$  NMR) to obtain structural and dynamic information about the effect of phloretin adsorption to a lipid bilayer.  $^2\text{H}$  NMR relaxation experiments were performed on SSVs, which allowed to estimate whether phloretin changes the lateral diffusion of lipid molecules (Bayerl and Bloom, 1990).

Up to now virtually no attention has been paid to possible variations of phloretin conformations and their dipole moments. Especially the variation of the latter may drastically affect the dipole potential at the lipid-water interface. A contribution to that issue is given by a computer-supported conformational analysis of phloretin. These calculations on the basis of energetic minimization provided conformers of the molecule in the gas phase and additional information about the probability of their occurrence on the basis of a Boltzman-weighting. Based on these conformers we included solvation effects within the semiempirical calculations. We were also able to determine the dipole moments of these phloretin conformations and to calculate the resulting dipole moment and its direction with respect to the structure of the molecule. These theoretically obtained data supported the experimental results concerning the interpretation of the molecular interaction of phloretin with membranes.

## 4.3 Materials and methods

### 4.3.1 Materials

DMPC and DMPC- $\text{d}_{13}$  were obtained from Avanti Polar Lipids (Alabaster, AL). Phloretin was obtained from Sigma (St. Louis, MO). Benzene was spectroscopically pure and ethanol was analytical grade (Merck, Darmstadt, Germany). Ultrapure water was obtained by passing deionized water through a Milli-Q equipment (Millipore, Bedford, MA). For the SSVs used at  $^2\text{H}$  NMR measurements silica beads of highest purity with a radius of  $200 \pm 50$  nm were used as solid support. SSVs for the measurements of phloretin adsorption was used as a commercially available kit Transil<sup>TM</sup> (Nimbus, Leipzig, Germany). The diameter of the silica beads was normally  $30 \mu\text{m}$ . The beads were non-covalently coated with egg-PC, with a surface area extent of  $10 \text{ m}^2/\text{g}$  beads.

### 4.3.2 Buffers and solutions

In DSC experiments, the samples were prepared by dissolving pure lipid (DMPC) or a mixture of lipid and phloretin in a mixture of benzene and ethanol (1:1 volume to volume ratio). After evaporation of the solvent in vacuum (12 h), the samples were incubated with buffer (0.1 M NaCl and 20 mM NaH<sub>2</sub>SO<sub>4</sub>) at a temperature well over the phase transition temperature and vortexed until a homogeneous emulsion was obtained. The lipid concentration of the DSC samples was 1.5 mg/ml buffer. The phloretin concentration was 50 mol % of the lipid. In DSC experiments the pH of the buffer was adjusted to 5, 7 and 9. In adsorption experiments phloretin was dissolved in 1 M NaOH and added to buffer (0.1 M NaCl and 20 mM NaH<sub>2</sub>SO<sub>4</sub>) for final concentrations between 10  $\mu$ M and 0.3 mM. The pH was adjusted to 5.5. SSVs were prepared by the vesicle fusion technique described in detail elsewhere (Naumann et al., 1992; Bayerl and Bloom, 1990). For the lipid/phloretin SSVs a lipid/phloretin solution (pH was adjusted to 7) was used of which the preparation was analogous to the DSC measurements. Adsorption experiments were performed at 22° C, NMR experiments at 30° C.

### 4.3.3 Differential scanning calorimetry (DSC)

High sensitivity DSC measurements were performed with a MC-2 microcalorimeter (MicroCal, North Hampton, MA). The calorimeter was interfaced to a personal computer and the data acquisition was controlled by this device. The scans for all measurements were done within a temperature range of 5 - 40° C, at a scan rate of 30° C/h and a 12 s time increment (filter constant). No significant differences in the DSC endotherms were observed for heating and cooling mode scans except for a small hysteresis. Data analysis was performed using the MicroCal Origin DSC analysis software package. Within the data analysis we standardized the raw data by baseline subtraction (Bayerl et al., 1988).

### 4.3.4 Measurement of phloretin adsorption

Silica beads coated with egg-PC bilayer were incubated in buffer containing various concentrations of phloretin. The lipid concentration was 0.18 mM. The beads were separated by centrifugation for 5 min at 10000  $\times$  g. Phloretin concentrations before incubation and after separation of the beads were determined by UV-spectroscopy at a wavelength of 285 nm using a Perkin-Elmer Lambda 2 UV/VIS spectrometer (Perkin-Elmer, Norwalk, CT). The linearity of the absorption units versus aqueous phloretin concentration was verified. Adsorption of phloretin was determined as the difference between its concentration in buffer before incubation and after separation of the beads and converted into molar ratios of phloretin adsorbed to lipid.

### 4.3.5 $^2\text{H}$ NMR measurement of SSVs

$^2\text{H}$  NMR measurements were performed at 76.7 MHz using a Bruker AMX 500 spectrometer equipped with a Bruker broadband high power probe with a 10 mm sample coil. A quadrupolar echo sequence with a CYCLOPS phase cycling scheme was used and the pulse length for a  $90^\circ$  pulse was  $5.5 \mu\text{s}$ . The repetition time was 300 ms and 2048 complex data points were collected in quadrature with a dwell time of  $5 \mu\text{s}$ . The spectra were obtained by a one dimensional Fourier transform starting at the top of the quadrupolar echo.

Longitudinal relaxation time  $T_{1z}$  measurements were performed by employing the inversion recovery pulse sequence and the  $T_{1z}$  values were obtained by analysis of the area of the spectra. For transverse quadrupolar echo relaxation time ( $T_{2e}$ ) measurements, the pulse spacing times  $\tau$  of the quadrupolar echo sequence were varied between 160 and 760  $\mu\text{s}$  and semilogarithmic plots of the peak echo intensity versus  $2\tau$  yielded linear dependencies of slope ( $T_{2e}^{-1}$ ). The calculation of the oriented  $^2\text{H}$  NMR spectra (bilayer normal parallel to the external magnetic field  $B_0$ ) was achieved by using an interactive de-packing program (Sternin et al., 1983). The residual second moment  $M_{2r}$  was calculated numerically from the corresponding spectrum  $f(\omega)$  according to the equation:

$$M_{2r} = \frac{\int_{-\infty}^{\infty} (\omega - \omega_0)^2 f(\omega) d\omega}{\int_{-\infty}^{\infty} f(\omega) d\omega} \quad (4.1)$$

### 4.3.6 Computational methods

The semiempirical AM1 (Dewar et al., 1985) and PM3 (Stewart, 1989) calculations for the gas phase as well as the AM1/SM5.2 calculations for solvent effects were performed on Silicon Graphics INDIGO (R4000) workstations using the VAMP 6.1 program (Rauhut et al.) and the program AMSOL (Hawkins et al.), starting from geometries preoptimized by the TRIPOS force field as implemented within the SYBYL program package. The conformational space of phloretin was searched semiempirically by varying the corresponding dihedral angles of the aliphatic chain and of the OH moieties and by the calculation of reaction coordinates using the corresponding keywords of the VAMP program package. For all conformers geometry optimizations were done by applying the EF algorithm with a gradient norm specification of  $0.1 \text{ mdyn}/\text{\AA}$ . The results of the AM1 gas phase calculations were taken as input geometries for the AMSOL program using the solvation model SM5.2 (solvent: water) and the default optimization algorithm implemented herein. The gradient norm was specified as  $0.45 \text{ kcal}/\text{\AA}$ . The *ab initio* calculations (6-31G\* basis set) were performed on the Fujitsu VPP700 supercomputer of the Leibniz Rechenzentrum in Munich using the Gaussian94 program package (Frisch et al., 1995).

## 4.4 Results

### 4.4.1 DSC with multilamellar lipid vesicles

DSC evaluation of lipid vesicles is highly sensitive to impurities and contaminations of the lipid and therefore a suitable method to determine interaction of phloretin with lipid in bilayers and multilayers. Fig. 4.2 shows DSC scans of DMPC MLVs in the absence and in the presence of 50 mol % phloretin. Pure MLVs exhibited a main phase transition temperature,  $T_m$ , of 23.6° C which is strictly independent on aqueous pH. Pretransition, caused by the transition from gel to rippled phase (Lee, 1977), occurred at 13.5° C. Any impurity which interferes with the packing of the lipid reduces  $T_m$  (Biltonen and Lichtenberg, 1993). Under the influence of phloretin,  $T_m$  is clearly reduced to 13° C at pH 5 (dashed line in Fig. 4.2), which indicates reduction of the lipid order, i.e., the entropy of the lipid is increased. This effect appeared to be pH dependent with a larger decrease of  $T_m$  the lower the pH was. At pH 7 (dotted line in Fig. 4.2) the phase transition temperature was 14° C, whereas  $T_m$  was about 14.5° C at pH 9.

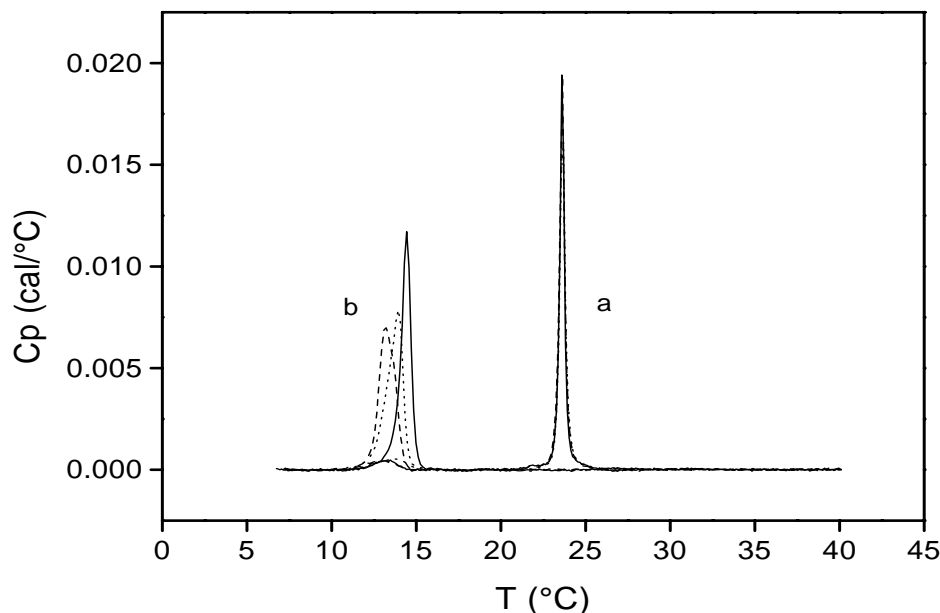


**FIGURE 4.2** DSC endotherms (excess heat capacity  $C_p$  versus temperature) of multilamellar DMPC lipid vesicles in the absence (a) and in the presence (b) of 50 mol % (of the lipid) phloretin at pH 5 (dashed lines), pH 7 (dotted lines) and pH 9 (full lines). The DSC scans were recorded in the heating mode. The curves of the scans in the absence of phloretin are nearly identical, so they appear as one. All curves are baseline-corrected.

This result is in agreement with earlier findings that only the neutral form of phloretin changes the properties of lipid monolayers and membranes (LeFevre and Marshall, 1959; Andersen et al., 1976, Cseh and Benz, 1998).

It is noteworthy, that the variation within the pH range between 5 - 9 caused a smaller effect on  $T_m$  than it would be expected having in mind that the concentration of neutral phloretin in water showed a drastic change in this pH range. At pH 5 nearly all phloretin molecules are neutral whereas only about 2% of the phloretin remains undissociated at pH 9 ( $pK_a = 7.35$ , Reyes et al., 1983). In contrast to this, the difference between  $T_m$  at pH 5 and pH 9 was much smaller than compared to that between pH 9 and the reference. This discrepancy may be explained by the preparation of the MLVs (see Materials and Methods), a thorough mixing of lipid and phloretin was ensured thus neutral phloretin was able to penetrate the inner layers of the MLVs. Only the outer layers are exposed to the bulk aqueous phase and respond to pH variation.

The results of the DSC measurements are summarized in Table 4.1. They clearly show that the phase transition temperature of pure DMPC was pH-independent. The addition of phloretin did not only change the phase transition temperature but also led to an increase of the width at halfheight  $T_{1/2}$ , which is related to the purity of the system and the cooperativity of phase transition.

**TABLE 4.1** Parameters calculated from the heat capacity - temperature data of the DSC measurements with DMPC multilamellar lipid vesicles in the presence (+) and in the absence (-) of 50 mol % phloretin at pH 5, 7 and 9. Phase transition temperature  $T_m$  and the width at halfheight  $T_{1/2}$  are the means  $\pm$ SD of at least 5 measurements.

pH	phloretin	$T_m$ ( $^{\circ}$ C)	$T_{1/2}$ ( $^{\circ}$ C)
5	-	$23.6 \pm 0.04$	$0.39 \pm 0.001$
5	+	$13.0 \pm 0.20$	$1.33 \pm 0.210$
7	-	$23.6 \pm 0.06$	$0.34 \pm 0.098$
7	+	$14.0 \pm 0.14$	$1.25 \pm 0.210$
9	-	$23.6 \pm 0.06$	$0.32 \pm 0.075$
9	+	$14.4 \pm 0.03$	$0.61 \pm 0.074$

The broadening of the endotherms appeared also to be somewhat pH dependent although we could not observe a systematic change. Bechinger and Seelig (1991) and Verkman and Solomon (1982) pointed out that phloretin has a high affinity to membranes, it partitions to a high degree to membranes without destabilizing the bilayer structure. The results of the DSC measurements derived from the experiments described here confirmed this. In spite of the comparatively strong decrease of lipid order indicated by the strong decrease of phase transition temperature in the presence of phloretin, the endotherms still showed relatively sharp peaks with moderate broadening. A much larger effect on the broadening of the endotherms has been reported from DSC measurements with similarly high doses of compounds mixed with the lipids such as cholesterol (Linseisen et al., 1993) and

myelin basic protein (Reinl and Bayerl, 1993). Phloretin appears therefore as a molecule, which adsorbs to a high degree to membranes but only slightly affects cooperativity of the lipids. Dehydration of the lipid head groups caused by phloretin adsorption as it has been proposed previously (Bechinger and Seelig, 1991), cannot be excluded here but is presumably not the only effect of lipid-phloretin interaction because of the strong decrease of the phase transition temperature  $T_m$ . Dehydration of lipids is usually accompanied by an increase of phase transition temperature (Heise et al., 1991; Kurrle et al., 1990).

It is noteworthy, that the endotherms of the DSC measurements in the presence of phloretin are nearly symmetric. An asymmetry would be an indication of either gel or liquid-crystalline region preference of the component integrated in the lipid layer (van Osdol et al., 1992; Ben-Yashar et al., 1987). Obviously phloretin does not exhibit any distribution preference to a certain phase state. The results of the DSC measurements are in good agreement with those of surface pressure versus molecular area isotherms of monolayers. Phloretin in its neutral form integrates also into monolayers and decreases the phase transition temperature (Cseh and Benz, 1999; see also paragraph 3.4.3).

#### 4.4.2 Computational calculation of the phloretin conformers

The semiempirical conformational analysis using the AM1 parametrization yielded the most stable conformations of the carbon skeleton 1A - 1D (Fig. 4.3). Except for the OH moiety next to the carbonyl group, which takes its stable arrangement by forming a hydrogen bond with the carbonyl oxygen, additional conformers are generated by rotating the OH groups about the adjacent C-O single bond. For these three hydroxy functions two minimum geometries were found, being the two possible arrangements in plane with the aromatic ring stabilized by hydrogen bonds between the oxygen atom and the aromatic hydrogens. Consequently, taking into account the orientations of the OH groups, each of the basic conformations 1A -1D split up into  $2^3 = 8$  conformers, denoted as a - h (Fig. 4.4). By semiempirical geometry optimization, all eight arrangements a - h with different heats of formations were found for the conformers 1A, 1C, and 1D (Table 4.2). In contrast, the basic geometry 1B remained stable only for the orientations a - d. The interaction of the flexible OH group in *ortho* position to the carbonyl function with the methylene moiety of the aliphatic chain as found in the conformations e - h obviously disturbed the nearly planar arrangement of the two aromatic rings in geometry 1B. Therefore, the total number of conformers found was 28 (instead of 32).

The dipole moments of the 28 conformers calculated with the AM1 parametrization vary over a wide range from 0.75 to 5.8 D, which mainly depends on the orientation of the OH moieties. These values were subjected to a Boltzmann-weighting based on the relative energies (heats of formation),  $\Delta H_f^0$ , of the conformers according to the equation

$$\frac{N}{N_0} = \exp \left( - \frac{\Delta \Delta H_f^0 4.1868 \times 10^3}{N_A k_B T} \right) \quad (4.2)$$

in which  $k_B$  is the Boltzman constant and  $T$  the temperature (295 K). The calculated contributions  $N/N_0$  of the discrete conformers  $N$  relative to the absolute minimum conformer  $N_0$  ( $= 1\text{Da}$ ) were normalized. By multiplication with the calculated dipole moments  $\mu$ , the contribution to  $\mu_{tot}$  of each conformer was obtained. Summation of these weighted contributions gave the overall dipole moment  $\mu_{tot}$  of phloretin. The results of the AM1 parametrization are summarized in Table 4.2. The calculated value of 3.25 D lies in the same order of magnitude as the calculated value found by Andersen et al. (1976), but is distinctly smaller by 40%. These calculations describe the properties of an isolated molecule in the gas phase. Interactions with solvent molecules, possibly stabilizing conformers bearing higher dipole moments, have been neglected. Switching to the PM3 parametrization (which is known to calculate electronic effects not properly) tended to calculate smaller discrete dipole moments and the Boltzmann-weighted value of 2.9 D is even lower than the result of the AM1 calculations.

The possible tautomerization of phloretin (1) to the enols 2 and 3 was taken into account by calculations on the conformers 2Da and 3Da (Table 4.2). The initial geometries of these molecules were generated from the absolute minimum conformer 1Da of the non-enolized phloretin (1). The AM1-calculated relative heats of formation of 2Da and 3Da are 13.2 and 18 kcal/mol (55.6 and 75.8 kJ/mol, respectively) higher than that of the non-enolized molecule 1Da. PM3 values of 14.9 and 21.7 kcal (62.7 and 91.4 kJ/mol, respectively) show the same tendency. When Boltzmann-weighted, due to their high energy content, the contribution of the enols 2 and 3 to the overall dipole moment is negligibly small. Consequently, no complete conformational analysis of the enols was carried out as the missing conformers were expected to be even more unstable.

To verify the higher energy contents of the enols, *ab initio* calculations using the RHF method and the 6-31G\* basis set were carried out (No dipole moments were calculated as this method neglects electron correlation). The resulting energetic separation of 14.58 and 24 kcal/mol (61.4 and 101 kJ/mol, respectively) for 2Da and 3Da confirms the semiempirical results and thus the instability of these tautomers compared with 1Da. We additionally performed semiempiric AM1-AMSOL calculations in order to estimate solvent effects. The conformers 1Aa - 1Dh and the enols 2Da and 3Da of the AM1 calculations were taken as the starting geometries for the program AMSOL. The implemented method generates a continuous space bearing the electrostatic properties of the chosen solvent around the input molecule, followed by the calculation of the energy of the molecule embedded in this solvent shell. Depending on the solvent, the order of the relative energies of different conformations may change, thus indicating (de)stabilization due to solvent effects.

Water as a polar and protic solvent was also chosen for our calculations. Compared with the results for the gas phase some of the conformers with higher dipole moments were slightly stabilized by the calculated influence of water. Consequently, the overall Boltzmann-weighted dipole moment of phloretin increased to 4.7 D. Since these values of the dipole moment of phloretin are calculated and differed by 40% from the published calculated value (Andersen et al. 1976; 5.6 D), we determined the dipole moment in

additional experiments using dioxan as the solvent. By measurements of the molar polarisation, molar refraction and density at different phloretin concentrations (data not shown) and extrapolation to infinite dilution (Hedestrand method), which corresponds to the gas phase, we estimated the dipole moment using the Debye and the Clausius-Mosotti equations (Exner, 1975; Minkin et al., 1970). The determined value was  $3.3 \pm 0.5$  D, which agrees very well with our calculated value for the gas phase (see Table 4.2).

**TABLE 4.2** Computational calculation of the relative heat of formation  $\Delta H_f^0$  and dipole moment  $\mu$  of the conformers of phloretin in the gas phase using the semiempirical AM1 parametrization. The conformer with lowest heat of formation (1Da) was defined to  $\Delta H_f^0 = 0$  the others were normalized to this. Based on the four stable conformations of the carbon skeleton 1A - 1D rotation of the OH-groups gave the conformers 1Aa - 1Ah, 1Ba - 1Bd, 1Ca - 1Ch and 1Da - 1Dh of the ketonic form. The calculation of the enolic forms 2Da and 3Da was based on the starting geometries of 1Da. The table also shows the contribution by Boltzmann statistics and the corresponding contribution to the total dipole moment  $\mu_{tot}$ . For details, refer to the text.

Conformer	rel. $\Delta H_f^0$ (kcal/mol)	contribution by Boltz- mann statistics (%)	$\mu$ (D)	contribution to $\mu_{tot}$ (D)
1Aa	0.629	4.815	2.354	0.113
1Ab	0.730	4.060	3.760	0.153
1Ac	1.368	1.382	3.969	0.055
1Ad	1.513	1.082	5.796	0.063
1Ae	3.014	0.086	0.822	7.053e-4
1Af	3.062	0.079	1.769	1.400e-3
1Ag	3.167	0.066	1.902	1.260e-3
1Ah	3.283	0.054	3.912	2.131e-3
1Ba	0.663	4.546	1.696	0.077
1Bb	0.720	4.129	3.830	0.158
1Bc	0.413	6.934	3.351	0.232
1Bd	1.495	1.116	5.401	0.060
1Ca	0.012	13.65	3.109	0.424
1Cb	0.023	13.40	2.878	0.386
1Cc	0.744	3.965	4.483	0.178
1Cd	0.762	3.846	4.691	0.180
1Ce	2.255	0.309	1.780	5.502e-3
1Cf	2.270	0.301	0.750	2.260e-3
1Cg	2.379	0.251	2.896	7.261e-3
1Ch	2.397	0.243	2.812	6.839e-3
1Da	0.000	13.92	2.329	0.324
1Db	0.047	12.86	3.432	0.442
1Dc	0.734	4.033	4.242	0.171
1Dd	0.787	3.867	4.843	0.179
1De	2.226	0.325	0.842	2.733e-3
1Df	2.221	0.327	1.659	5.431e-4
1Dg	2.352	0.262	2.567	6.736e-3
1Dh	2.364	0.257	3.098	7.966e-3
1				$\sum = \mu_{tot} = 3.245$
2Da	13.20	3.381e-11	5.314	0.000
3Da	18.00	1.026e-14	4.172	0.000

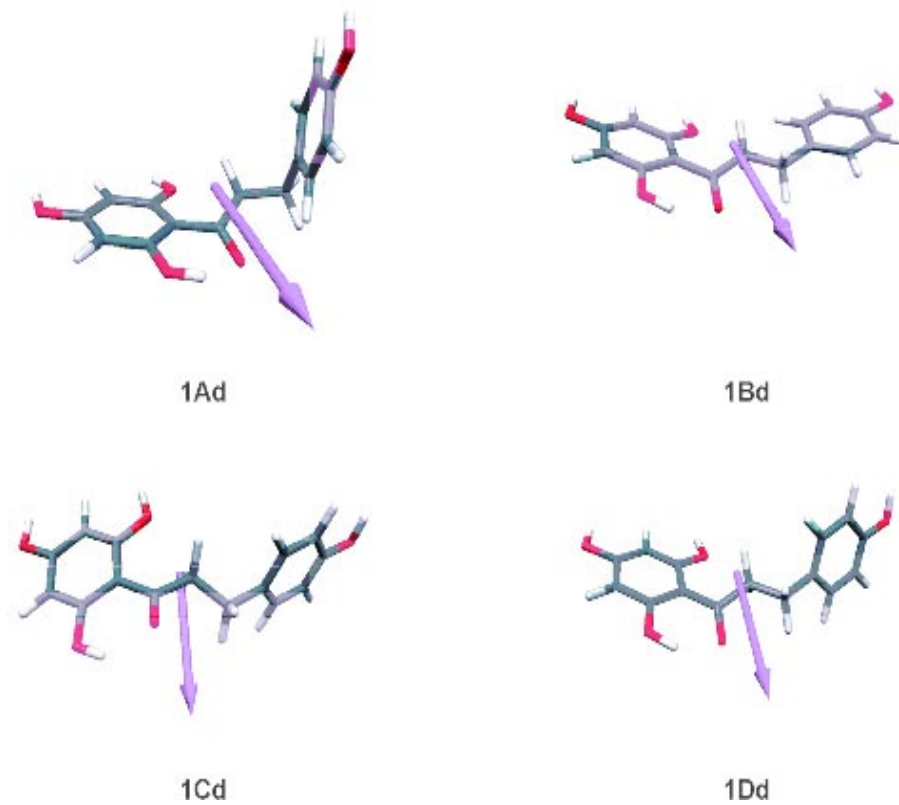


**FIGURE 4.3** Phloretin conformers in the gas phase as calculated by the semiempirical AM1 parametrization. Each of the conformers 1Ad - 1Dd represents an example of the basic conformations of the ketonic form. The arrows indicate the dipole moment vectors, their lengths are proportional to the corresponding calculated dipole moments.

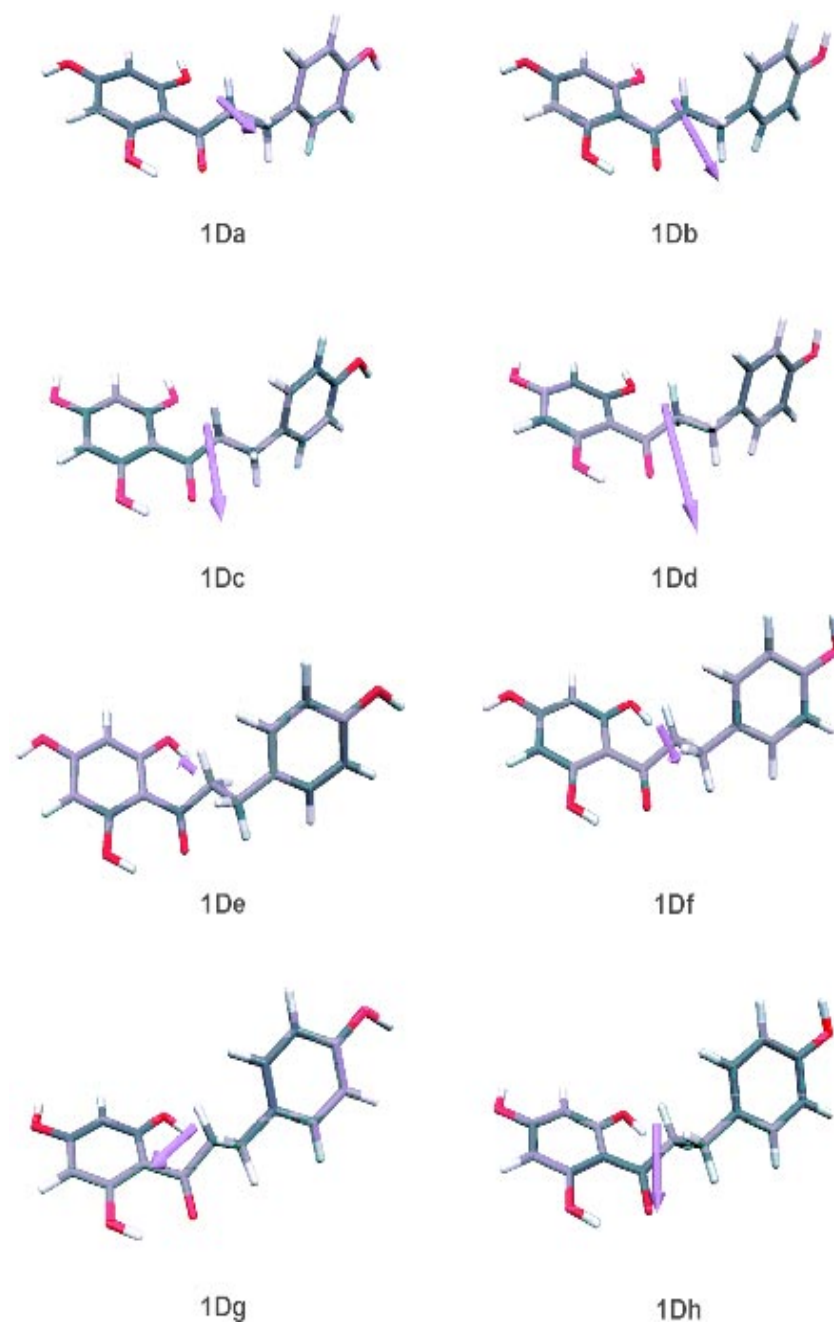


**FIGURE 4.4** Phloretin conformers in the gas phase as calculated by the semiempirical AM1 parametrization. The basic conformer 1D is shown in all stable arrangements a - h. The arrows indicate the dipole moment vectors, their lengths are proportional to the corresponding calculated dipole moments.

### 4.4.3 Adsorption isotherm of phloretin to SSV

Adsorption of phloretin to monolayers and membranes is usually described by a Langmuir adsorption isotherm (De Levie et al., 1979; Reyes et al., 1983). This means that the surface density of adsorbed molecules,  $\Gamma$ , is dependent on the aqueous concentration,  $c$ , and converges to a saturation limit at high concentrations. The maximum surface density,  $\Gamma_\infty$ , and the dissociation constant,  $k$ , are the characteristic parameters of the Langmuir adsorption isotherm, which can be described according to Eq. 2.1 (see paragraph 2.3).

In this study we determined the adsorption of phloretin to lipid bilayers in a direct way measuring the concentration of phloretin in buffer before and after adsorption to SSV. Solid supported bilayers (SSV) (Bayerl and Bloom, 1990) are suitable for this purpose since they can easily be separated by centrifugation and permit therefore, rather than pure lipid vesicles (Verkman and Solomon, 1982), an easy spectrophotometric determination of the concentration of phloretin in the aqueous phase. Phloretin in its undissociated form has an absorption peak at a wavelength of 285 nm. Fig. 4.5A shows the adsorption isotherm of phloretin to egg-PC bilayers on a solid support dependent on the aqueous concentration of phloretin. Adsorption is given as the molar ratio of phloretin adsorbed to lipid. The Langmuir fit yielded a maximum molar ratio of 0.3 (which corresponds to a maximum phloretin surface density,  $\Gamma_\infty$ , of approximately  $43 \mu\text{mol}/\text{m}^2$  as calculated from the surface area of the lipid on the SSV) and a dissociation constant,  $k$ , of  $49 \mu\text{M}$ .

Another appropriate way to determine  $k$  is to refer to the dipole potential change,  $\Delta\Psi$ , which accompanies the adsorption of phloretin to lipid monolayers and bilayers (Andersen et al., 1976; Cseh and Benz, 1998). The change in dipole potential of monolayers and bilayers as a function of the surface density of adsorbed molecules bearing a dipole moment, such as phloretin, can be described according to Eq. 3.1 (see paragraph 3.4.4). Detailed descriptions of the adsorption model are given at paragraph 2.3 and elsewhere (De Levie et al., 1979; Reyes et al. 1983; Cousin and Motais, 1978; Cseh and Benz, 1998). According to Eq. 3.1  $\Delta\Psi$  is a linear function of the dipole surface density, therefore the corresponding maximum surface density can be expressed by the maximum potential change,  $\Delta\Psi_\infty$  (Eq. 2.3, see paragraph 2.3).

Fig. 4.5B shows the dipole potential change of phloretin to egg-PC bilayers dependent on the aqueous concentration of phloretin (The phloretin-induced change in dipole potential of black lipid bilayer membranes was estimated from its influence on dipicrylamine transport parameters in charge-pulse experiments; see paragraph 2.5.2). The fit according to Eq. 2.3 yielded a maximum potential change of 164 mV and a dissociation constant of  $9 \mu\text{M}$ . Both values agree well with those that have been found by Reyes et al. (1983) ( $\Delta\Psi_\infty = 200 \text{ mV}$ ,  $k = 7 \mu\text{M}$ ).

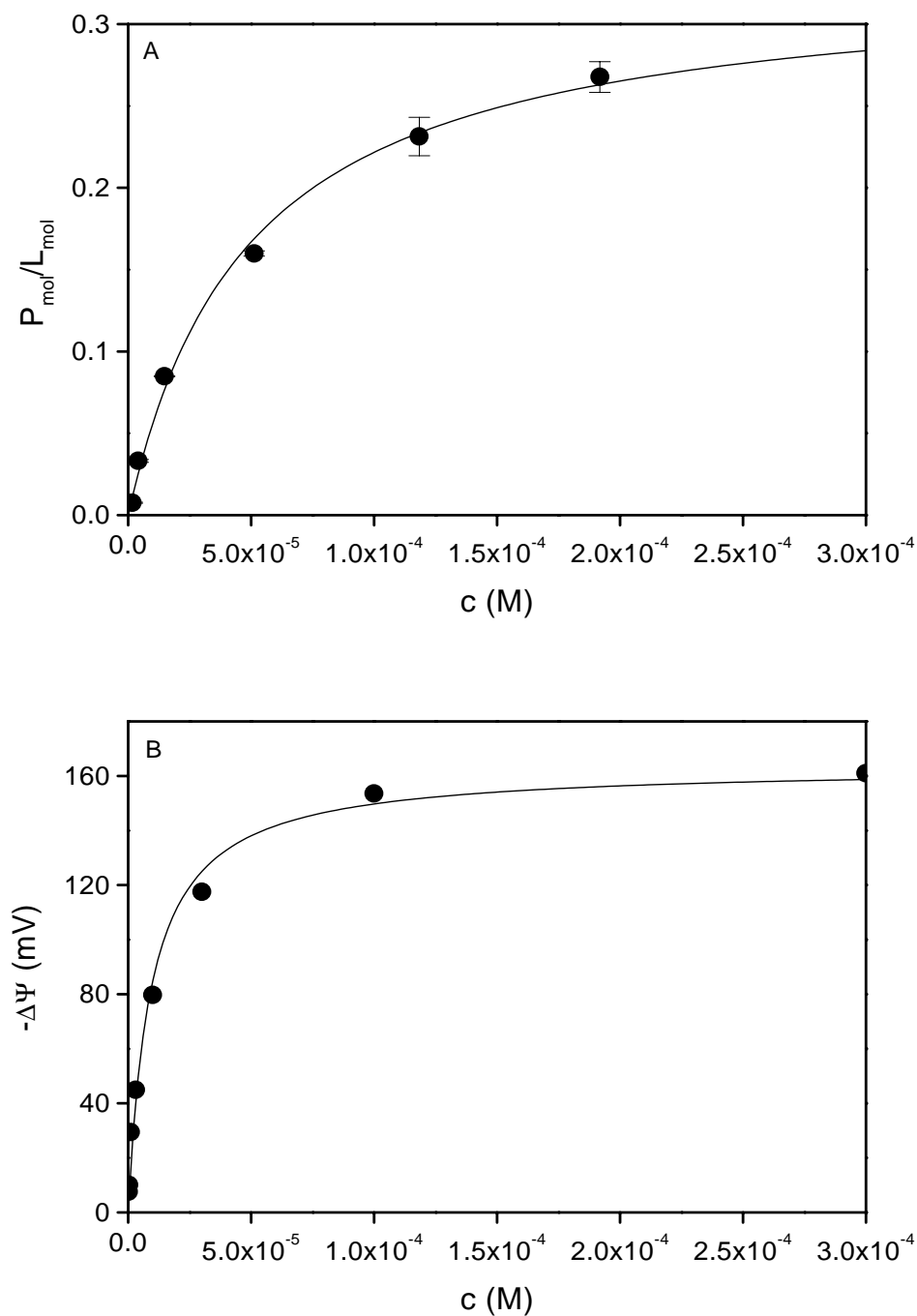


**FIGURE 4.5** (A) Adsorption of phloretin to egg-PC bilayers on a solid support denoted as the molar ratio adsorbed phloretin/lipid,  $P_{\text{mol}}/L_{\text{mol}}$ , versus the aqueous phloretin concentration. The data are fitted according to the Langmuir adsorption isotherm (Eq. 2.1) where instead of the surface density,  $\Gamma$ , the molar ratio is used for the calculation. (B) Change of dipole potential,  $\Delta\Psi$ , of egg-PC black lipid membranes versus aqueous phloretin concentration obtained from charge-pulse experiments with the lipophilic ion dipicrylamine. The data were fitted according to Eq. 2.3. In both experiments the aqueous phase contained 100 mM NaCl and 20 mM  $\text{NaH}_2\text{PO}_4$ , the pH was 5.5 and

the temperature was 22° C. The standard deviations were below  $\pm 10$  mV. For details refer to the text.

With both methods it can be shown that the adsorption of phloretin saturates with increasing aqueous concentration and that the data can be fitted according to the Langmuir adsorption isotherm (According to the improved model in paragraph 2.3 the fit of the data shown in Fig. 4.5B exhibited a  $\Delta\Psi_\infty$  of 188 mV and a  $k$  of 4.31  $\mu\text{M}$ . However, for the purpose in this section, the accuracy of the fit in Fig. 4.5B is sufficient.). Independent of the different methods the parameters of the Langmuir adsorption isotherm should correspond with one another. It is impossible to calculate the surface density of phloretin from  $\Delta\Psi$  because of the unknown parameters that determine  $\Delta\Psi$  (Eq. 3.1). Thus, we cannot compare the values of maximum adsorption but it is possible to derive the dissociation constant,  $k$ , which represents a meaningful number for the affinity of phloretin to the lipid. The values of  $k$  derived from Figs. 4.5A and 4.5B, however, differ by a factor of about 5 using the two different methods. Differences in the same order of magnitude were also found for experiments with phloretin analogs (data not shown). This considerable discrepancy cannot be explained by statistical dispersion of the experimental data alone, but must be caused by the functional relationship between the dipole potential determining parameters. The dipole potential change is related to the surface density according to Eq. 3.1, that means, any variation of the involved parameters influences  $\Delta\Psi$ . A surface density dependent variation of one or more parameters in Eq. 3.1 might be an explanation of the different value of  $k$  determined by the dipole potential change measurements (Cseh and Benz, 1998; see also Discussion, paragraph 4.5).

#### 4.4.4 $^2\text{H}$ NMR with unilamellar lipid vesicles on a spherical support (SSV)

The adsorption of phloretin to membrane surfaces suggests that it interacts mainly with the phospholipid head groups (Bechinger and Seelig, 1991; Cseh and Benz, 1999). To study this possible interaction in more detail, we performed  $^2\text{H}$  NMR measurements with phloretin and the head group deuterated lipid DMPC- $\text{d}_{13}$ . Fig. 4.6, lower panel, shows a comparison of the  $^2\text{H}$  NMR spectra of DMPC- $\text{d}_{13}$  SSVs without (dotted line) and with (solid line) 50 mol % phloretin. The upper panel of Fig. 4.6 demonstrates the corresponding de-paked oriented spectra without (dotted line) and with (solid line) phloretin. When the motional freedom of the headgroup moieties is considered it is possible to assign the quadrupolar splitting of 1025 Hz to the nine protons in the three methyl groups of choline for the spectrum without phloretin. Similarly that of 5.6 kHz could be designated to that of the  $\alpha$  and  $\beta$  segments of the head group, which could not be separated in the absence of phloretin. Phloretin has a considerable effect on the  $^2\text{H}$  NMR spectra of DMPC- $\text{d}_{13}$  SSVs. Its incorporation resulted in quadrupolar splittings of 733 Hz for the methyl groups and 7.3 and 2.2 kHz for the  $\alpha$  and  $\beta$  methylenes, respectively. This result can be understood by geometrical considerations, if we assume that phloretin is indeed localized within the polar head groups. Similarly, the tendency of increased splitting for the  $\alpha$  segment and de-

creased splitting for the  $\beta$  segment has previously been reported for POPC multilamellar vesicles, when phloretin is present (Bechinger and Seelig, 1991). Additionally, we measured a decrease of the splitting of the methyl groups, which is a result of the same effect. It has previously been reported for negatively charged molecules/amphiphiles that their addition to a lecithin bilayer changes the orientation of the  $^-P-N^+$  dipole from nearly parallel to the membrane surface to an orientation more towards the hydrocarbon phase (Scherer and Seelig 1989). It is obvious that a similar effect was here observed for the incorporation of phloretin in the SSV.

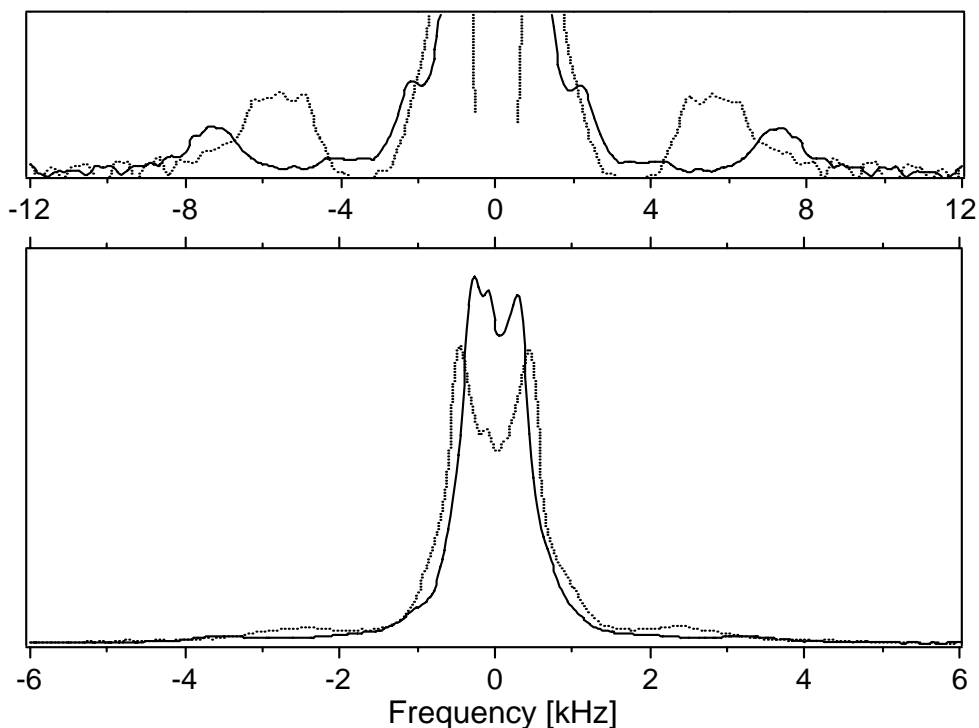


**FIGURE 4.6**  $^2H$  NMR spectra of DMPC- $d_{13}$  SSVs at  $30^\circ C$  without (dotted line) and with (solid line) 50 mol % phloretin. Bottom panel: powder spectra. Top panel: calculated oriented spectra.

We measured spin lattice relaxation of the choline head group to investigate the changes of the headgroup dynamics as a result of the incorporation of phloretin. The results of these experiments are summarized in Table 4.3. We found similar  $T_{1z}$  values without ( $23.2 \pm 0.7$  ms) and with ( $22.9 \pm 0.3$  ms) 50 mol % phloretin.  $T_{1z}$  is sensitive to fast motions in the Larmor frequency regime and therefore the results give no indication for an altered head group dynamics in the frequency range of the quadrupolar resonance when phloretin is present.

For curved bilayers the dominating relaxation mechanism in NMR measurements is lateral diffusion of the phospholipids (Sternin et al. 1983; Köchy and Bayerl, 1993) and the diffusion correlation time is defined by  $t_D = R^2/6D$ , where  $D$  is the lateral diffusion constant and  $R$  is the radius of the curvature. We investigated the transverse relaxation time  $T_{2e}$ , which has been shown to be sensitive to motions that are slow on the NMR time

scale  $t_M$  (here  $t_M = 1/\sqrt{M_{2r}} = 9.3 \times 10^{-5}$  s obtained from the residual second moment  $M_{2r}$  of the pure DMPC-d<sub>13</sub> bilayer). In the slow motion limit of  $t_D \gg t_M$  and for a separation  $t$  in the two-pulse echo experiment of  $t \gg t_M$ , the  $T_{2e}$  time is proportional to  $t_D$  (Pauls et al., 1985), i.e., a slower lateral diffusion would yield a slower transverse relaxation rate. In the fast motion limit  $t_D \ll t_M$  the relaxation rate,  $1/T_{2e}$ , is proportional to the residual second moment  $M_{2r}$  (Pauls et al., 1985), thus an increased  $M_{2r}$  would lead to a faster transverse relaxation.

**TABLE 4.3** Results of <sup>2</sup>H NMR spectroscopy measurements from line shape and relaxation experiments on DMPC-d<sub>13</sub> spherical supported unilamellar vesicles (SSV) with and without 50 mol % phloretin at pH 7.

SSV	$\Delta\nu_Q$ (Hz)			$T_1$ (ms)	$T_2$ ( $\mu$ s)	$M_{2r}$ ( $10^8$ s <sup>-2</sup> )
	CH <sub>3</sub>	$\beta$	$\alpha$			
without phloretin	1025	5600		23.3 $\pm$ 0.7	862 $\pm$ 45	1.18
with phloretin	733	2198	7255	22.9 $\pm$ 0.3	1402 $\pm$ 18	1.16

In our study we measured for the pure DMPC-d<sub>13</sub> SSVs  $T_{2e} = 862 \pm 45$   $\mu$ s and with phloretin  $T_{2e} = 1402 \pm 18$   $\mu$ s. Considering  $M_{2r}$  of all head group deuterons together the slow motion limit  $t_D \gg t_M$  is fulfilled. This result could mean that phloretin reduced the lateral diffusion of the lipids. However, if we assume the methyl moieties to dominate the measured  $T_{2e}$  relaxation time, then their  $M_{2r}$  can be calculated according to  $M_{2r} = 4\pi^2/5 \Delta\nu_Q^2$  giving  $t_M = 35 \times 10^{-5}$  s for the pure system and  $t_M = 49 \times 10^{-5}$  s with phloretin. In our study we used as a solid support silica beads with a diameter of 400 nm. For pure DPPC multilayers a diffusion constant of  $(12 \pm 1) \times 10^{-12}$  m<sup>2</sup>/s has been reported (Karakatsanis and Bayerl, 1996), which results in a diffusion correlation time  $t_D = 55 \times 10^{-5}$  s. This means that for both  $t_M$  values neither the fast nor the slow motion limit strictly applies ( $t_D = 55 \times 10^{-5}$  s) and thus the reduction in  $T_{2e}$  relaxation might be simply a result of the reduction in quadrupolar splitting and phloretin has a negligible influence on lipid diffusion along the silica beads.

## 4.5 Discussion

### 4.5.1 Interaction of phloretin with lipids in membranes

The results of the DSC measurements clearly demonstrated that phloretin decreases the phase transition temperature of lipid membranes. This effect is dependent on the concentration of its neutral form in the lipid phase and indicates that phloretin integrates into the membrane and changes the lipid packing (Biltonen and Lichtenberg, 1993). However, a pure hydrophobic interaction between the lipid and phloretin, i.e., its simple integration into the hydrophobic interior of the membrane cannot be supported by our DSC study.

Despite the high degree of integration as judged by the strong decrease of the phase transition temperature, the endotherms show only weak broadening indicating that the cooperativity of lipid phase transition is hardly affected. In contrast to this the integration of hydrophobic molecules into the hydrocarbon region of the lipid layer affects strongly the cooperativity of phase transition and leads to a large broadening of the endotherms (Reinl and Bayerl, 1993). A pure electrostatic interaction with the lipid headgroups is also unlikely because the typical increase of phase transition temperature mediated by this type of interaction is also missing (Reinl and Bayerl, 1993; Dluhy et al., 1983; Cevc et al., 1981). Lipid monolayer experiments on a Langmuir trough (Cseh and Benz, 1999; see also paragraph 3.5.3) have shown that phloretin affects lipid packing, but this effect is counterbalanced by increasing surface pressures, leading to a gradual squeezing out of phloretin at higher surface pressures. Simultaneous monitoring of the dipole potential change, however, has been demonstrated that phloretin remains adsorbed to the monolayer. Therefore, the interaction of phloretin with lipids seems to be restricted to that within the headgroups, which suggests that phloretin molecules integrated into the lipid layer are preferentially localized within the headgroup region. The DSC experiments with MLV described here confirm the monolayer results. Another indication of the preferential location of phloretin within the headgroups has been given by Bechinger and Seelig (1991). In their NMR-study the order of the hydrocarbon chains in POPC membranes remains almost unaltered whereas the headgroup orientation is considerably changed by phloretin.

### 4.5.2 Phloretin conformers and their dipole moments

In chapter 2 we have shown that the adsorbed dipoles influence one another, when their density is large enough. As a consequence the adsorption of dipole molecules does not follow any longer the Langmuir adsorption isotherm (Cseh and Benz, 1998). It is also possible that the adsorbed dipoles have an influence on the conformation of the further adsorbed dipole molecules. The calculation of the stable phloretin conformers revealed a wide distribution of possible dipole moments. We therefore cannot refer to phloretin as a molecule with a clearly defined dipole moment with respect to the effects on the dipole potential of monolayers and membranes. Neither we cannot proceed with the assumption that the conformers all show the same lipid affinity and behave as one single molecule. These aspects get some importance when we try to correlate the reduction of the dipole potential at the adsorption of phloretin with the size of its overall dipole moment. Reyes et al. (1983) have found in their study that the dipole moments of phloretin and its analogs roughly correlate with the dipole potential change but they also have observed exceptions of this rule. They have concluded that the change in dipole potential is not a simple function of the dipole moment of the adsorbed molecule but is highly dependent on the number and position of the hydroxyl groups in the ring and the surface density in the membrane. Having in mind the large variation of the dipole moments of the phloretin conformers calculated here and their strong dependence on the orientation of the OH-

moieties, it is possible that the dipole moments of adsorbed molecules are different from the overall dipole moment of molecules in the aqueous phase and, moreover, they may indeed change their conformation when they adsorb to the lipid layer thereby changing their dipole moment.

In most of the studies that have been published so far phloretin is described as a molecule bearing a large dipole moment, which is responsible for the dramatic change of the dipole potential of monolayers and membranes. Our estimation of the overall dipole moment both calculated and experimentally found qualifies the correlation between the dipole moment of phloretin and its dipole potential reducing effect. The dipole moment vector of phloretin is mainly determined by the orientation of the carbonyl oxygen and the OH groups. The direction of the dipoles, as derived from the calculations of the conformers, is predominantly perpendicular to the longitudinal axis of the molecule. The calculated and experimentally found value of the dipole moment of phloretin in this study was about 40% smaller than described in literature. This result suggests that the role of the dipole moment of phloretin when adsorbed to lipid layers has been overestimated previously. This also means that the structure of the dipole molecules has a more important function than expected.

### 4.5.3 Parameters of phloretin adsorption to membranes

The results of our adsorption experiments with phloretin clearly demonstrated that a considerable difference exists between the dissociation constants determined here and those obtained from dipole potential measurements. The critical difference between these two methods is that the latter one is only able to properly describe adsorption of a dipole molecule if it is accompanied by a dipole potential change. Moreover, adsorption usually has been described using a static electrical model, which means that the relation between the surface density of phloretin molecules adsorbed to the lipid layer and the dipole potential change is supposed to be linear (Reyes et al., 1983; De Levie et al. 1979). However, this assumption is only valid when the parameters involved in Eq. 3.1 are taken as constants and do not depend on the surface density or on the dipole potential change. We have demonstrated (see chapter 2) that the dipole potential of a membrane represents a considerable driving force for the adsorption of a dipolar molecule to the membrane (Cseh and Benz, 1998). This means that the entire driving force for adsorption of such a molecule can be splitted in a part that represents the Langmuir interaction and a part which is dependent on the existing dipole potential of a membrane and therefore decreases with the decrease of total dipole potential of the lipid layer. The observed difference between the dissociation constants derived from the dipole potential change and the adsorption of phloretin to the SSV can be explained if we take into account the relation between the dipole potential as a driving force and the alignment of the adsorbed dipoles as its effect. If we assume that the dipoles of the adsorbed molecules can change their direction and their dipole moment they will respond to the preexisting potential with uniform alignment opposite to the electric field and therefore decrease the dipole potential of membranes

and monolayers. Consequently, at a certain surface density of adsorbed molecules the total dipole potential of the lipid layer will reach a very small value close to that where the dipoles of further adsorbed phloretin molecules will be randomly aligned and do not contribute to  $\Delta\Psi$  any more. This means that the change of dipole potential caused by the adsorption of phloretin to membranes strictly depends on the preexisting potential. Our adsorption model previously proposed (see chapter 2) takes account of this by separating the Langmuir and the dipole-dipole interaction. Following this approach we conclude that even if the value of  $\Delta\Psi$  is close to the maximum value  $\Delta\Psi_\infty$  and saturates at a given phloretin concentration, a further adsorption according to the Langmuir interaction may still be possible. As a consequence the dissociation constant calculated from the change of the dipole potential and from the direct adsorption experiments differ considerably as shown here. Furthermore, we have to conclude that adsorption isotherms obtained from measurements of the dipole potential change are able to describe the electrical aspects of adsorption of a dipole molecule to lipid membranes. However, they do not allow a proper description of the Langmuir interaction if their adsorption at high surface density of molecules it is no longer accompanied by a change of dipole potential. This means that the dipole moments of adsorbed phloretin molecules must not be regarded as static quantities because of the heterogeneous dipole moment distribution of the various conformers, they may change dependent on their surface density.

Verkman and Solomon (1982) have investigated the permeation of phloretin through lipid bilayers and found in their study that although the binding of phloretin to a lipid membrane is a saturable process, the permeation kinetics appear to be unsaturable. The same result has recently been reported by Pohl et al. (1997). Verkman and Solomon (1982) have suggested two binding sites with different affinities for phloretin to account for this phenomenon. Pohl et al. (1997) have proposed that phloretin adsorption and transmembrane permeation should be considered as competitive events. This means that prior to phloretin permeation no adsorption at the interface is required. They assumed that in contrast to adsorbed phloretin, which reduces the dipole potential, diffusing phloretin is randomly aligned and therefore not detectable by means of dipole potential measurements. However, although we neither found indications of multiple binding sites on the basis of our own adsorption measurements nor favor a model which treats adsorption and permeation as processes that are independent of each other, it seems reasonable to distinguish different states of phloretin at the water-lipid interface in particular at high surface densities when the phloretin-mediated dipole potential decrease is considerable. This means that the dipole moments normal to the interface of adsorbed phloretin molecules may differ from each other. Different conformers may well account for the discrepancies between adsorption and permeation that have been described previously (Pohl et al., 1997; Verkman and Solomon, 1982).